Phenolic acids interactions with clay minerals: A spotlight on the adsorption mechanisms of Gallic Acid onto montmorillonite

Adoum Mahamat Ahmat, Thomas Thiebault, Régis Guégan

Phenolic acids interactions with clay minerals: a spotlight on the adsorption mechanisms of Gallic Acid onto Montmorillonite

Adoum Mahamat Ahmat[(a,b)1], Thomas Thiebault[(c)], Régis Guégan[(b,d) 2]

(a) *Institut Mines-Telecom Lille-Douai, Department of Civil Engineering and Environment. 764, Boulevard Lahure, 59508 Douai, France.*

(b) *Institut des Sciences de la Terre d'Orléans ISTO, UMR 7327, University of Orléans, 1A Rue de la Férollerie, 45500 Orléans La source, France.*

(c) *EPHE, PSL University, UMR 7619 METIS (SU, CNRS, EPHE), 4 place Jussieu, F-75005, Paris, France*

(d) *Faculty of Science and Engineering, Global Center for Science and Engineering, Waseda University, 3-4-1 Okubo, Shinjuku-ku, Tokyo 169-8555, Japan.*

Abstract

For a better understanding of the preservation of organic matter in clay minerals, the adsorption of a model humic substance, the Gallic Acid (GA), onto a Na-montmorillonite (Na-Mt) was performed in batch situation for various experimental conditions (pH=2, 5, 7) in order to mimic the natural context. The adsorption efficiency and change in the clay mineral were characterized *via* a set of complementary experimental techniques (Fourier transform infrared spectroscopy, X-ray diffraction, elemental analyses). Adsorption isotherms at the equilibrium were fitted with the models of Langmuir, Freundlich and Dubinin-Radushkevitch allowing one to precisely quantify the adsorption through the derived fitting parameters. From the adsorption data combined with complementary results of the modeled humic-clay complexes, different types of interactional mechanisms were inferred as a function of background acidity: (i) at pH=2 while protonated GA was the preponderant form, anionic GA species can be adsorbed to the Na-Mt surface through electrostatic interaction, leading to the a

[1] Corresponding author. *E-mail address*: adoum.mahamat-ahmat@bordeaux-inp.fr (A. Mahamat Ahmat).
[2] Corresponding author. *E-mail address*: regis.guegan@aoni.waseda.jp (R. Guégan).

slight covering of the clay surface favoring in a second step the GA adsorption by π-π and Van der Waals forces; XRD patterns corroborated via TGA and FT/IR results suggested the actual intercalation of the phenolic acid within the interlayer space; (ii) At pH = 5, above the pKa of phenolic acid, only 20% of the protonated form subsisted and these species were adsorbed via coordinative bonding, without however any perceptible intercalation; (iii) and in the regime with neutral environment (pH=7), the preponderance of GA anionic species led to a poor adsorption which appeared to be only located at the external surface of the clay mineral.

Keywords: Phenolic acids; Montmorillonite; Adsorption; Organic matter preservation.

1. Introduction

Clay minerals were recognized to stabilize soluble organic compounds through the adsorption of dissolved OM in superficial horizons of soils (Gonzalez, 2002; Kögel-Knabner et al., 2008; Schmidt et al., 2011; Kaiser et al., 2016). The confinement of organic compounds within the interlayer space of clay minerals avoids any heterotrophic reactions and leads to their preservation (Kaiser and Guggenberger, 2007; Wattel-Koekkoek and Buurman, 2004). It also favors the generation of polymeric macromolecules *via* the condensation of single monomers (Stevenson, 1982; Wang et al., 1983; Yariv and Cross, 2002). From the numerous research works on the subject, and more particularly studies focusing on the understanding of the interaction between clay minerals and humic substances leading to the formation of humic-clay complexes, it appears that simple blocks of polymeric humic molecules or elementary monomolecular compounds play a major role in the interaction with the mineral surface and stabilization of the complexes (Greenland, 1971; Feng et al., 2005; Wang and Xing, 2005; Chotzen et al., 2016; Chen et al., 2017).

The typology of physicochemical mechanisms allowing the establishment of perennial association between organic compounds and mineral surfaces were extensively studied in recent years. For example, ligand exchanges and cationic exchanges are reported as sustainable organo-mineral interaction mechanisms (Keil and Mayer 2014; Lambert, 2018), while low energy bonding such as van der Waals effects and hydrogen bonding are acknowledged to establish easily reversible associations (Plante et al., 2005; Lutzow et al., 2006). Aqueous media chemistry strongly constrains the preponderance of these mechanisms (Arnarson and Keil, 2000). Background parameters as ionic strength and pH shape clays' state of charge as well as the degree of protonation of dissolved organic compounds. Hence, it impacts the type of adsorption driving process. Chen et al., 2017 stressed out higher

47 adsorption performances of humic compounds onto 2: 1 clay minerals at low pH and
48 suggested the increase of electrostatic phenomena to explain this observation.

49 Besides background properties, organic compounds intrinsic characteristics also
50 determine the extent of the adsorption and constrain the nature of preponderant bonding
51 mechanisms (Bu et al., 2017). In the presence of compounds with different spatial structures
52 and molecular functions, a competition to the occupation of adsorption sites can occur. For
53 example, the adsorption of amino acids onto montmorillonites is more effective than the
54 uptake of phenolic acids contained in the same aqueous mixture (Gao et al., 2017).
55 Understanding these mechanisms is mandatory to assess the potential use of clay minerals in
56 the adsorption of contaminants of various natures. Clays and clay minerals are investigated
57 raw, or after chemical modification, as an economically viable removal pathway of petroleum
58 by-products (Meleshyn and Tunega, 2011; Lamishane et al., 2016) and emerging
59 pharmaceutical molecules (Li et al., 2011; Thiebault et al., 2015; De Oliveira et al., 2017)
60 commonly encountered in hydrographic networks. The uptake performance may be boosted
61 via inorganic pillaring (Liu et al., 2015) or surfactant intercalation (De Oliveira and Guégan
62 2016).

63 Thus, the study of the fundamental mechanisms of organo-mineral aggregation has
64 applications in various fields. In this paper, the emphasis is placed on the organo-clay
65 association, and its further protective role. This role has been assessed in sedimentary
66 environments through different approaches (Kennedy and Wagner, 2011; Arndt and
67 Jorgensen, 2013; Mahamat Ahmat et al., 2016, 2017). It appeared that organo-clay
68 associations involving ionic exchanges and those resulting from interlayer intercalation
69 allowed efficient isolation against microbial stresses. In pedological context, the mechanism
70 has mainly been studied from the perspective of complex polymeric humic acids (Chen et al.,
71 2017; Derakhshani and Naghizadeh, 2018).

While the main interaction mechanisms ensuring the stability of the organo-mineral complexes are rather difficult to determine in the case of humic substances (Tombácz et al., 2004; Chotzen et al., 2016; Chen et al., 2017), this research work aims at characterizing precisely the main driving force leading to the aggregation of OM. For this purpose, we focus on a simple carboxylic acid (gallic acid) as simple blocks or monomeric components in polymeric humic acids. Gallic Acid (GA) is a phenolic acid found in vascularized plants, inputted in soil horizons as single molecules or apart of large polyphenolic macromolecules such as tannins and various ligno-cellulosic by-products. Here, in this research work, we focus on the sorption mechanisms of GA onto montmorillonite under different experimental conditions.

2. Materials and methods

2.1. Interaction of the carboxylic acids with a clay mineral

A natural Wyoming Na-montmorillonite (Na-Mt) was supplied by the Source Clay Minerals Repository of the Clay Minerals Society. Its structural formula can be expressed as: $(Ca_{0.12}Na_{0.32}K_{0.05})$ $[Al_{3.01}Fe(III)_{0.41}Mn_{0.01}Mg_{0.54}Ti_{0.02}]$ $[Si_{7,98}Al_{0.02}]$ $O_{20}(OH)_4$. Gallic Acid (GA) was provided from Sigma Aldrich at 97.5 % purity grade and was used without further treatment. This weak acid can be seen as a phenolic compound owing a carboxylic function with 2 alcohol groups (Fig. 1). Its physico-chemical parameters (topological surface, pKa) are summarized in Table 1.

The interactions between GA and Na-Mt were conducted in different experimental conditions under various pH conditions: 2, 5 and 7. Typically, the adsorbent mass was 150 mg in 50 mL solution spiked with a GA concentration between 10 mg. L^{-1} and 2 g. L^{-1}. The pH value was adjusted with both NaOH and HCl solutions (0.1 M). The solutions were stirred at 200 rpm with a magnetic stirrer during 24 hours in order to reach the equilibrium (kinetic data not shown) at room temperature. The solid fraction (*i.e.* organo-clay complexes) was

separated from the liquid one through a centrifugation step (5000 rpm; 10 min) and then lyophilized before flash pyrolysis analyses.

2.2. Experimental Techniques

Adsorbed organic carbon was measured using flash pyrolysis (Thermo Scientific Flash 2000 organic analyzer) performed on organo-clay complexes in powder form.

The samples were also characterized *via* Fourier Transform Infrared Spectroscopy (FT/IR) in the range 650-4000 cm^{-1}. Measurements were realized using a Thermo Nicolet 6700 FT spectrometer equipped with a Deuterated Triglycine Sulfate (DTGS) detector at room temperature and for different temperatures controlled by a Linkam thermal device allowing us to characterize the thermal behavior on a wide range of temperature: 50-550°C. The analyses were performed in transmission mode and each spectrum corresponded to the average of 256 scans collected at 2 cm^{-1} of resolution.

The d_{001} spacing's of the organo-mineral complexes was determined by the first *00l* reflection from the X-rays patterns which were recorded on a conventional θ-θ Bragg-Brentano configuration by using a Thermo Electron ARL'XTRA diffractometer equipped with a Cu anode (CuK_{α} = 1.5418 Å) coupled with a Si(Li) solid detector. The diffractograms on dry samples (100°C for 24 h) were performed between 1 and 24° (2θ) with an angular and time steps of 0.04° and 10 s, respectively.

Thermal gravimetric analyses were carried out under atmospheric conditions at the heating rate of 10 °C min^{-1} from room temperature (25°C) to 800 °C using the thermal gravimetric analyzer (Model: STA PT 1600, manufactured by Linseis Company, Germany).

2.3. Sorption Modeling

The fitting of the resulting adsorption isotherms by using Langmuir, Freundlich and Dubinin–Radushkevich (DR) equation models drive to numerous thermodynamic parameters allowing to precisely quantify the affinity of GA with the Na-Mt. Briefly, Langmuir model assumes

that the whole organic molecules are adsorbed on singularized sites on the accessible surface of the adsorbent, and each site hosts a unique molecule. This Langmuir model is expressed by the following equation (LeVan and Vermeulen, 1981):

$$q_e = q_{max} K_L / [1 + (K_L C_e)] \quad (1)$$

where q_e is adsorbed amount when equilibrium is reached (mol g^{-1}); C_e is the remaining concentration in the solution at equilibrium (mol L^{-1}); q_{max} is the maximum sorption capacity of the Na-Mt, and K_L is the Langmuir constant (L mol^{-1}) which is related to Gibbs free energy $\Delta G°$ (kJ mol^{-1}) through the thermodynamic equation (2):

$$\Delta G° = -RT \ln K_L \quad (2)$$

where R represents the universal gas constant (8.314 J mol^{-1} K^{-1}) and T the temperature (K).

Freundlich and D-R equations takes into account surface heterogeneities on the adsorption process and deal with the variabilities in the interaction mechanisms leading to the adsorption of organic compounds that can form or be organized in multi-layers. Freundlich adsorption model is a linear relation (LeVan and Vermeulen, 1981; Özcan et al., 2005) expressed through the following equation:

$$\ln q_e = \ln K_F + 1/n (\ln C_e) \quad (3)$$

Where K_F ($g\ L^{-1}$) and n are constants and indicate respectively the extent of the adsorption and the degree of non-linearity between GA and the smectite. Indeed, when the term $1/n$ ranges between 0.1 and 1, it suggests that the adsorption mechanism is favorable (Liu et al., 2011). D-R isotherms allow one to acquire complementary thermodynamic parameters. Its equation is written as:

$$\ln q_e = \ln q_m + \beta * \varepsilon^2 \quad (4)$$

Where ε is the Polanyi potential, computed through the relation (5)

$$\varepsilon = RT \ln (1+1/Ce) \quad (5)$$

q_m is the theoretical potential saturation capacity of the sorbent and β is the constant related to the activity ($mol^2\ J^{-2}$) connected to the mean free energy E of adsorption ($kJ\ mol^{-1}$) via the equation (6):

$$E = 1 / \sqrt{2\beta} \quad (6)$$

This later parameter gives information whether the adsorption mechanism involves a cation exchange or physical adsorption. Indeed, if the magnitude of E is below 8 $kJ\ mol^{-1}$, physisorption is envisaged, while for $E > 8\ kJ\ mol^{-1}$ the adsorption process follows an ion exchange or a chemisorption mechanism.

Moreover, we used an error function (F_{error}) in order to evaluate which equation model was best suited to describe these processes. A lower result from the error function indicated a smaller difference between adsorption capacity calculated by the model ($q_{i\ cal}$) and the experimental ($q_{i\ exp}$). F_{error} can be expressed according to the following Eq. (7)

$$F_{error} = \sum (q_{i\ cal} - q_{i\ exp} / q_{i\ exp})^2 \quad (7)$$

Where $q_{i\ cal}$ is a value of q predicted by the fitted model; $q_{i\ exp}$ is a value of q measured experimentally; i indicates the values of the initial GA concentration of the experiments; and P is the number of experiments performed.

3. Results and discussions

3.1. pH dependence on the adsorption of GA onto Na-Mt

The adsorption isotherms at the equilibrium stress out the actual affinity of GA with Na-Mt (Fig. 2). Indeed, adsorption isotherms display a gradual growth of the adsorbed amount

when the equilibrium concentration increases. The slope of this growth attenuates at high starting concentrations emphasizing a saturation state, excepted for the isotherm realized at pH=5.

GA adsorption isotherms are properly fitted by the three equation models used as r^2 values display values between 0.95 and 0.99 and F_{error} values are between 0.0010 and 0.130 for GA (Table 2). Based on r^2 values, experimental data seem to be better adjusted to the Langmuir model, however its function errors are higher than 0.1 and to those for both Freundlich and DR equations, which spread out from 0.001 to 0.004. This is a side effect of the logarithmic scale adopted in Freundlich and DR representations. Although Langmuir equation properly fitted experimental data, the two latter equations appear to be more suitable for modeling the adsorption of the phenolic acid onto the clay mineral surface. Indeed, clay mineral shows a heterogeneous surface leading to a distribution of several adsorption sites that are taken into account in both Freundlich and DR equation models.

Under low pH conditions (*i.e.* below the pKa of GA), the adsorption is particularly enhanced, with the predominance of the protonated form of GA (*i.e.* acidic form) in solution, due to the decrease of the repulsion between the neutral GA and Na-Mt. However, the situation may be rather twisted with antagonist effects. Indeed, under such pH conditions (pH=2), the pH value is lower than the pH of zero net proton charge (pH_{ZNPC}) of Na-Mt, estimated about 4.5 (Tombàcz and Szekeres, 2006). For $pH < pH_{ZNPC}$, the electric charge of the edge-sites of clay mineral surface changes from anionic to cationic, favoring the adsorption of phenolic acids in their anionic form, (*i.e.* base) allowing a possible ion exchange process which enhances the amount of adsorbed organic acids. In contrast, at pH=5 and 7, since both the clay mineral edge-sites and the equilibrium ratio between the acid/base forms change (Fig. 3), the adsorption involves additional interactional mechanisms, affecting the lineshape of the

adsorption isotherms while reducing the adsorbed amounts. This lowering is due to the repulsion between anionic charges of both GA and Na-Mt.

Fig. 4 shows the X-ray diffraction patterns evolution of the GA-clay complexes (dried for 48 hours at 100°C to prevent any water molecules in the interlayer space that may interfere in the interpretation and understanding of a possible intercalation of the GA) following the starting GA concentration. The diffraction patterns display several diffraction peaks located between 5° and 9° (2θ) related to the 00*l* reflections. At pH=2, the *00l* reflection shifts to lower angle values, attesting the effective intercalation of the phenolic compound. As well, it is interesting to remark the narrowing of these reflections suggesting an enhancement of the organization in the layered material probably due to the increase of the GA density within the clay–GA complexes. The basal spacing of GA-Mt complexes (*i.e.* d_{001}), estimated with the angular position of the *00l* reflection, increases from 9.6 Å for a dehydrated clay mineral to about 13.3 Å at pH=2. While an intercalation occurs at low pH, this phenomenon is not observed for the other two pH, where a slight increase of the interlayer space to a value of 11 Å can be noticed (Fig. 5). This is probably due to both the clay mineral charge density and the preponderance of the neutral (RCO_2H) form which play an important role in the adsorption as well its associated interaction mechanism (*e.g.* coordinative bonding).

The contribution of FT/IR spectroscopy gives important information in the characterization of GA-clay complexes derived from GA and Mt and confirms its actual adsorption. Absorption bands observed at 1350, 1384 and 1470 cm^{-1} are assigned to stretching modes of C – O. and bending modes of C-H of O-H respectively (Fig. 6). The strong vibration at 1700 cm^{-1} was assigned to C=O stretching of GA's carboxylic function. Besides the existence of a drift or a temperature gradient in temperature during the FT/IR experiments, the complete degradation of GA is accomplished at relative high temperature in contrast to bulk

GA which is decomposed at about 300°C estimated through thermal gravimetric measurements (Fig. 8). This last observation about the preservation of GA at high temperature is related to its confinement within the interlayer space of Mt obtained for GA at pH=2.

TG analyses allow assessing the loss of weight of the adsorbent during a gradual heating. Organo-clay minerals display usually three main weight losses during the heating. The first one is associated to the evaporation of free and adsorbed water, ranging between the initial temperature and 150°C. The second one is related to the thermal oxidation of adsorbed organic compounds between 150 and 600°C with a maximal decomposition temperature related to the characteristics of organic moieties. Finally, for temperatures higher than 600°C, only the dehydroxylation of clay minerals is expected (Xie et al., 2001). Fig. 8 gathers TG and DTG curves of GA-Na-Mt composites. Weight losses associated to the dehydration remains independent from pH values. Corresponding DTG peaks occur between 98 and 105°C. With growing temperature, the distinction between each sample is more pronounced. Hence, between 150 and 600°C, no significant weight loss is displayed at pH=7, whereas noteworthy weight losses are observed at the lower pH values (2 and 5). The first decomposition temperature is noticed at 247°C and corresponds to the decomposition of acidic group of GA (Rao et al., 1981; Hussein et al., 2009). In the organic matter combustion range, GA-Na-Mt complexes aggregated at pH = 5 display one loss of weight (*i.e.* 340°C), while those formed at pH=2 exhibit two noticeable losses at 310 and 410°C (Fig. 8). This splitting after interaction at pH=2 might be explained by the distinction between GA adsorbed onto the external surface of the clay mineral (*i.e.* lower temperature) and intercalated GA (*i.e.* higher temperature) (Zhu et al., 2017). Hence, this result appears to be consistent with XRD results, in which an intercalation of GA only occurs after interaction at pH=2.

3.2. Adsorption mechanisms and geochemical model of GA-Mt complexes

The observation that GA adsorption is higher at pH < pKa is in agreement with the results of Rabiei et al., 2016 which stressed out higher GA adsorptions at pH=3 (33%) compared to their experiments performed at pH=7 (20%). This pH-dependency is related to the protonation capacity of GA's polar appendage (COOH / COO^-). It must be noted however, that the pH control of GA adsorption cannot be generalized to the interaction of other phenol-based molecules. The study by Dolaksis et al., 2018 for instance, suggested that the adsorption of phenolic cores devoid of polarizing COOH appendix is pH–independent. They showed that low energy mechanisms (hydrogen bridges) drive the adsorption of chlorophenols and nitrophenols onto silicate surfaces.

At a pH < pKa, GA is mainly protonated (neutral) and this form represents about 99.6 % of the chemical species at pH=2 (Fig. 3). However, in acidic condition, the charge density of the edge-sites of Na-Mt changes and switches below the pH of zero net proton charge estimated at 4.5 (Table 1). Here, despite the possibility of an alteration of the structure and probably the chemical composition of the layered material, the adsorption of GA appears to be enhanced in acidic conditions. The parameters derived from the fitting procedure, and more particularly those of the D-R model giving a free energy of adsorption *E* slightly above 8 kJ mol^{-1}, underlining the possibility of chemical process for adsorption or at least strong electrostatic interactions. Although being less known and implied in the adsorption of anionic compounds onto Mt, electrostatic interaction was recognized as the main driving force leading to the intercalation of various kind of anionic compounds: tannic and benzoic acids, anionic surfactants (Yan et al., 2007; Zhang et al., 2012; An and Dultz 2007), that may occur nevertheless, in particular experimental conditions (low pH range) as it is the case here. Moreover, the increase of the basal spacing of Na-Mt after the interaction with GA at pH=2 (i.e. + 3.7 Å) is consistent with the molecular size of GA (i.e. z=3.7 Å, Figure 1), emphasizing the possible intercalation of GA through a horizontal monolayer within Na-Mt layers.

265 The adsorption of anionic species, even weak, acts as a coating that may favor further
266 adsorption of organic molecules as organoclay materials do, nevertheless cannot only explain
267 the totality of the adsorbed amount reaching about 1.5 x 10^{-4} mol g^{-1}. Indeed, GA is in anionic
268 form at a low concentration. The amount of anionic species may increase during the sorption
269 mechanism since the uptake involves the displacement of acid basic equilibrium. This may
270 allow *in fine* the adsorption of higher amount of anionic species. However, the effect of this
271 acid basic shift is limited. Protonated species of GA remain preponderant and are likely to be
272 adsorbed through other bonding mechanisms. Since GA is mainly neutral at pH < pKa as
273 explained before, its adsorption should be driven through physisorption mechanisms such as
274 molecular interaction (π- π interaction, van der Waals forces) with the prior adsorbed
275 molecules and by coordinative bonding through inorganic exchangeable cations located
276 within the interlayer space and with the carboxylic moieties as both FT / IR and XRD data
277 highlighted. A recent work stressed out the importance of ion-dipole interaction (a
278 coordinative bonding mechanism) as the main driving force for the adsorption of nonionic
279 surfactants (Guégan et al., 2017) onto a Mt surface and can be according to previous studies
280 in the literature (Sonon and Thompson, 2005; Deng et al., 2006) extended to nonionic
281 compounds and here GA in its neutral form (Fig. 7).

282 The preponderance and the role of this interaction is confirmed at a pH value of 5 where
283 the maximum adsorbed amounts at the equilibrium reaches 1.3 x 10^{-4} mol g^{-1}. Based on the
284 diagram of preponderance of GA species in regards to pH, its neutral form represents about
285 20% at a pH=5 (Fig. 3). The experiment with the highest starting concentration of 2 g L^{-1}
286 leads to 5.88 x 10^{-4} mol g^{-1} (if one does the hypothesis that such amount is adsorbed – number
287 of GA moles normalized to the mass of Mt introduced) where 20% are in the RCO_2H form
288 (neutral one), thus driving to a value of 1.176 x 10^{-4} mol g^{-1}, close to the experimental one
289 estimated at 1.3 x 10^{-4} mol g^{-1}. At this pH value, the clay mineral displays a cation exchange

capacity as well as an anionic charge surface increasing the repulsion between adsorbent and organic anions. Hence, the protonated form of GA is favored for adsorption, and may interact to the inorganic exchangeable cations through coordinative bonding forces. However, it is important to mention that 20% of the inorganic exchangeable cations are located onto the external surface of the clay mineral (Swartzen-Allen and Matijević, 1975; Shainberg et al., 1980; Patzko and Decany, 1993; Logdson and Laird, 2004), where they can be easily mobilized for a cation-exchange or other interactions such as coordinative bonding or other mechanism such as cationic bridges involving the anionic species and divalent compensating cations. Here, the adsorption of GA does not lead to any intercalation as the XRD data displayed and exclusively remains on the external surface. The presence of the inorganic exchangeable cations at about 20% of the CEC on the external surface can be easily mobilized through coordinative bonding or via complexation reactions (Fig. 7) with the phenolic acid of which adsorbed amount match a value lesser than the 20% of the CEC (1.6×10^{-4} mol g^{-1}).

Similar observations are noticed at pH=7, where the adsorbed amount of neutral GA is not enough to lead to any intercalation as both XRD (Fig. 5) and FT/ IR data showed and restrict at this pH range principally anionic species in the adsorption. Indeed, in contrast to the previous pH, where the proportion of neutral species of GA represents about 96 and 20 % at pH=2 and 5 respectively, at a pH=7, it is insignificant with only 0.25 % (Fig. 3). While, the anionic form of GA is preponderant, an adsorption is surprisingly observed without however any intercalation as it was the case for pH=5, leading to an adsorbed amount of about 1×10^{-4} mol g^{-1} (Fig. 2). Here, the adsorption may involve interaction mechanisms such as cationic bridges between anionic GA and divalent inorganic cations. Hence, even mostly compensated with Na^{+}, around 20% of the compensating inorganic cations of Na-Mt are Ca^{2+}, that are able to sorb anionic species through cationic bridges (Errais et al., 2012; Thiebault et al., 2016; Rabiei et al., 2016). It should be mentioned that this mechanism could also play a key-role at

315 pH = 5, although the distinction between these mechanisms is not possible based on these
316 experiments (Fig. 7).

317 *3.3 Putting into perspective the behavior of GA with other phenolic-based compounds*
318 *and clay minerals*

319 The adsorption of GA is enhanced at low pH, as polyphenolic humic molecules behave
320 (Feng et al., 2005; Zhang et al., 2012; Chotzen et al., 2016). Polyphenolic molecules as fulvic
321 and humic acids, exhibit indeed greater adsorption rates with growing acidity (Gouré-Douby
322 et al., 2018). For instance, the study of Chen et al. (2017) focusing on the adsorption of soil
323 macromolecular humic acids onto both montmorillonite and kaolinite, pointed out the
324 enhancement of the adsorption at low pH. GA adopts a similar behavior when background pH
325 ranges below its pKa and allows a preeminence of its protonated species.

326 In the case of natural polyphenolic molecules (humic substances), it has been repeatedly
327 observed that in addition to background acidity, the nature of the adsorbent has a predominant
328 role. Clay minerals of the 1:1 group such as kaolinite appear more conducive to the adsorption
329 of humic –type of polyphenols. This is promoted by edges electrostatic phenomena. The
330 extent of the adsorption through edge electrostatic interaction principally depends on the
331 physico-chemical properties and mineralogy of a clay mineral, and more particularly its pH of
332 zero net proton charge (pH_{ZNPC}) which is estimated to 4.5 for Na-Mt (Tombàcz and Szekeres,
333 2006), lower than other soil clayey components such as kaolinite (Wiliams and Wiliams,
334 1978; Gupta and Miller, 2010). With its particular properties: a pH_{ZNPC} and background
335 protonation leading to a proper dispersion of clay mineral particles, kaolinite favors the
336 adsorption of macromolecular humic acids at large content in contrast to Na-Mt besides its
337 large CEC and specific surface area values (Chotzen et al., 2016). With similar background
338 chemistry, GA is likely to mimic the behavior of such soil poly-phenolic compounds. Since
339 sorbent's charge distribution varies according to clayey groups; mineralogical typology must

be added to the key criteria ruling GA's adsorption However, care should be taken in comparing the uptake of these phenolic-based compounds as differences in molecular masses, spatial arrangements and number of charges may induce differences in sorptive behaviors.

Although being poorer from quantitative perspective, the interaction of GA with Na-Mt remains interesting from a protective point of view since its neutral form may intercalate (Fig. 2; Fig. 7) under specific acidic conditions (pH < pKa). Interlayers isolations are reported to reduce bioavailability (Theng et al., 2001) and help to prevent biotic redox transformations.

In our case, the pH dependence of the adsorption appears to be consistent with the trends shown by other phenolic and polyphenolic molecules. However, the nature of the interactional mechanisms varies according to the molecules and does not display any systematic pattern. Although our results suggest intercalation and surface complexations via weak mechanisms (coordinative bonding), ligand exchanges are often involved in the interaction of long phenolic chains.

This encourages to complexify our view of the aggregation modalities of clays and phenol-like molecules and the possibility of organic matter stabilization process that it inducts. Na-Mt interactional mechanisms seems to differ whether the involved organic molecule are heavy macromolecular acids or singularized phenolic compounds. Thus, in a pedological environment where micro-fauna regime induces high rates of polymeric lyses and solubilizes a high quantity of phenolic acids, the stabilization process follows a different pathway from the configuration where polymeric humic acids are weakly degraded. In the first case, our data suggest that intercalation should prevail during the adsorption of poly-phenolic acids by-products in acidic pH conditions, while several studies point out adsorption on the edge and ligand exchanges in the ecological context where polymeric forms are preserved (Feng et al., 2005; Zang et al., 2012; Chotzen et al., 2016; Chen et al., 2017).

4. Conclusions

The series of organo-clay interactions performed here under evolutionary batch equilibrium conditions allowed to characterize the adsorption mechanisms of GA, a common phenolic acid in natural pedological media, onto Na-Mt. The parameters derived from fitting of GA data with a reasonable agreement (high r^2 values) to the adsorption models used: Langmuir, Freundlich and D-R equations, gave pertinent insights for a proper description of the phenomena under different approaches which pointed out the good affinity of the phenolic acid to Na-Mt. Additional experimental results obtained by FT/IR, TGA and XRD corroborated the actual adsorption of GA onto Na-Mt.

From the set of data, it appears that this monomolecular acid is mainly adsorbed through coordinative bonding interaction in contrast to macromolecular humic acids at low pH range, where ligand exchanges or complexation reaction occur according to the literature. Here, GA, a singularized element of large pedological compounds, interacts with the clayey mineral mainly via both surface and interlayer processes at low pH, leading to its confinement within the interlayer space which may allow a sustainable preservation of the organic matter in that way.

Acknowledgement

This study was supported by the project MONITOPOL funded by the French region Centre Val de Loire (grant number 00117247). The authors are grateful to Marielle Hatton for her analytical contribution.

Figures Captions

Fig. 1: Chemical structure of Gallic Acid (GA).

386 Fig. 2: Adsorption isotherms of Gallic Acid. Beige squares represent the data obtained at pH
387 2, green ones are for the data measured at pH 5 and the red triangles represent those collected
388 at pH 5. The continuous line represents Langmuir model fit.

389 Fig. 3: GA speciation following pH conditions.

390 Fig. 4: Graph of the 3D evolution of XRD diffraction patterns of dehydrated Gallic Acid (GA)
391 and Na-Mt composite samples as a function of the starting GA concentrations in solution for
392 pH=2. Only the results going up to 0.1 g L^{-1} are presented here, since no particular evolution
393 of *(001)* planes was observed beyond this concentration.

394 Fig. 5: Evolution of the d_{001} basal spacing determined by the 00l reflection of Na-Mt layers
395 obtained for GA / Na-Mt humic-clay like samples.

396 Fig. 6: FT/IR spectra of GA/Na-Mt composite samples (pH=2): thermic evolution.

397 Fig.7: Schematic representation of the possible adsorption mechanisms leading to the
398 intercalation of GA within the interlayer of a Na-Mt at pH=2, and adsorption for the pH=5
399 and 7.

400 Fig. 8: TG (solid lines) and DTG (dashed lines) curves of GA/Na-Mt (C_{GA} = 0.1 g L^{-1})
401 composite samples after interaction at pH=2 (dark gray lines); pH=5 (dark lines) and pH=7
402 (light gray lines).

403 **Tables Captions**

404 Table 1: Physico-chemical properties of implemented clay mineral (Na-Mt) and GA.

405 Table 2: Adsorption isotherm constants determined with Langmuir, Freundlich, and Dubinin-
406 Radushkevich model fit for the adsorption of GA onto Na-Mt for different pH.

407 **Supplementary data**

408 Appendix 1: Spectroscopic observations (FT/IR) of GA-Na-Mt complexes aggregated at
409 different levels of GA starting concentrations.

410 **References**

411 An, J-H., Dultz, S., 2007. Adsorption of tannic acid on chitosan-montmorillonite as a function
412 of pH and surface charge properties. Applied Clay Science 36, 256-264.

413 Arnarson, T.S., Keil, R.G., 2000. Mechanisms of pore water organic matter adsorption to
414 montmorillonite. Marine Chemistry 71, 309-320.

415 Arndt, S., Jorgensen, B.B., 2013. Quantifying the degradation of organic matter in marine
416 sediments: A review and synthesis. Earth-Science Reviews 123, 53-86.

417 Bu, H., Yuan, P., Liu, H., Liu, D., Liu, J., He, H., Li, Z. (2017). Effects of complexation
418 between organic matter (OM) and clay mineral on OM pyrolysis. Geochimica et
419 Cosmochimica Acta, 212, 1-15.

420 Chen, H., Koopal, L.K., Xiong, L.K., Xiong, J., Avena, M., Tan, W., 2017. Mechanisms of
421 soil humic acid adsorption onto montmorillonite and kaolinite. Journal of Colloid and
422 Interface Science 504, 457-467.

423 Chotzen, A.R., Polubesova, T., Chefetz, B., Mishael, Y.G., 2016. Adsorption of soil-derived
424 humic acid by seven clay minerals, a systematic study. Clays and Clay Minerals 64,
425 628-638.

426 De Oliveira, T., Guegan, R., 2016. Coupled Organoclay / Micelle Action for the Adsorption
427 of Diclofenac. Environmental Science & Technology 50, 10209-10215

428 De Oliveira, T., Guégan, R., Thiebault, T., Le Milbeau C., Muller F., Teixeira, V., Giovanela,
429 M., Boussafir, M., 2017. Adsorption of Diclofenac onto organoclays: effect of
430 surfactant and environmental (pH and temperature) conditions. Journal of Hazardous
431 Materials 323, 558-566.

Deng, Y., Dixon, J.B., Norman White, G., 2006. Bonding mechanisms and conformation of poly(ethylene oxide)-based surfactants in interlayer of smectite. Colloid and Polymer Science 284, 347-356.

Derakhshani, E., Naghizadeh, A., 2018. Optimization of humic acid removal by adsorption onto bentonite and montmorillonite nanoparticles. Journal of Molecular Liquids 259, 76-81.

Dolaksiz, E.Y., Temel, F., Tabakci, M., 2018. Adsorption of phenolic compounds onto calix[4]arene-bonded silica gels from aqueous solutions. Reactive and Functional Polymers 126, 27 - 35.

Errais, E., Duplay, J., Elhabiri,M., Khodja, M., Ocampo, R., Baltenweck-Guyot, R., Darragi,F., 2012. Anionic RR120 dye adsorption onto raw clay: Surface properties and adsorption mechanism. Colloids and Surfaces A: Physicochemical and Engineering Aspects 403, 69 - 78.

Feng, X., Simpson, A.J., Simpson, M.J., 2005. Chemical and mineralogical controls on humic acid sorption to clay mineral surfaces. Organic Geochemistry 36, 1553-1566.

Gao, J., Jansen, B., Cerli, B., Helmus, R., Mikutta, R., Dultz, S., Guggenberger, G., Kalbitz, K., 2017. Competition and surface conditioning alter the adsorption of phenolic and amino acids on soil minerals. European Journal of Soil Science 68, 667-677.

Gonzalez, J- M., 2002. Role of clay minerals on soil organic matter and humification. Ph.D thesis of Iowa State University, 212 pp.

Gouré-Douby, H., Martias, C., Smith, A., Villandier, N., Sol, V., Gloaguen, V., Feuillade, G., 2018. Adsorption of fulvic and humic like acids on surfaces of clays: Relation with SUVA index and acidity. Applied Clay Science 154, 83-90.

455 Guégan, R., Veron, E., Le Forestier, L., Ogawa, M., Cadars, S., 2017 Structure and dynamics
456 of nonionic surfactant aggregates in layered materials. Langmuir 33, 9759-9771.

457 Gupta, V., Miller, J.D., 2010. Surface force measurements at the basal planes of ordered
458 kaolinite particles. Journal of Colloid and Interface Science 344, 362-371.

459 Greenland, D.J., 1971. Interaction between humic and fulvic acids and clays. Soil Science,
460 111 34-41.

461 Hussein, M.Z.B., Ghotbi, M.Y., Yahaya, A.H., Abd Rahman, M.Z., 2009. Synthesis and
462 characterization of (zinc-layered-gallate) nanohybrid using structural memory effect.
463 Materials Chemistry and Physics 113, 491-496.

464 Kaiser, K., Guggenberger, G., 2007. Sorptive stabilization of organic matter by microporous
465 goethite: Sorption into small pores vs. surface complexation. European Journal of Soil
466 Science 58, 45-59.

467 Kaiser, K., Zederer, D.P., Ellerbrock, R.H., Sommer, M., Ludwig, B., 2016. Effects of
468 mineral characteristics on content, composition, and stability of organic matter fractions
469 separated from seven forest topsoils of different pedogenesis. Geoderma 263, 1-7.

470 Keil, R.G., Mayer, L.M., 2014. Mineral matrices and organic matter. Treatise on
471 Geochemistry (Second Edition) 12, 337-359.

472 Kennedy, M.J., Wagner, T., 2011. Clay mineral continental amplifier for marine carbon
473 sequestration in a greenhouse ocean. Proceedings of the National Academy of Sciences
474 of the United States of America 108, 9776-9781.

475 Kögel-Knabner, I., Guggenberger, G., Kleber, M., 2008. Organo-mineral associations in
476 temperate soils: Integrating biology, mineralogy, and organic matter chemistry. Journal
477 of Plant Nutrition and Soil Science-Zeitschrift für Pflanzenernahrung und Bodenkunde
478 171, 61-82.

Lambert, J.F., 2018. Organic pollutants adsorption on clay minerals. Developments in Clay Science 9, 195-253.

Lamishhane, S., Bal Krishna;K.C., Sarukkalige, R., 2016. Polycylic Aromatic Hyrdrocarbons (PAHs) removal by sorption: A review. Chemosphere 148, 336-353.

LeVan, M.D., Vermeulen,T., 1981. Binary Langmuir and Freundlich isotherms for ideal adsorbed solutions. The Journal of Physical Chemistry 85, 3247-3250.

Li, Z., Chang, P-H., Jiang. W-T., Jean, J-S., Hong, H., Liao, L., 2011. Removal of diphenhydramine from water by swelling clay minerals. Journal of Colloid and Interface Science 360, 227-232.

Liu, R., Zhang, B., Mei, D., Zhang, H., Liu, J., 2011. Adsorption of methyl violet from aqueous solution by halloysite nanotubes. Desalination 268, 111-116.

Liu, Y., Dong, C., Wei, W., Yuan, W., Li, K., 2015. Adsorption of levofloxacin onto an iron-pillared montmorillonite (clay mineral): Kinetics, equilibrium and mechanism. Applied Clay Science 118, 301-307.

Logsdon, S.D., Laird, D.A., 2004. Electrical conductivity spectra spectra of smectites as influenced by saturating cation and humidity. Clays and Clay Minerals 52, 411 – 420.

Lutzow, M., Kögel-Knabner, I., Ekschmitt, K., Matzner, E., Guggenberger, G., Marschner, B., Flessa, H., 2006. Stabilization of organic matter in temperate soils: Mechanisms and their relevance under different soil conditions-A review. European Journal of Soil Science 57, 426-445.

Mahamat-Ahmat, A., Boussafir, M., Le Milbeau, C., Guégan, R., Valdès, J, Guiñez, M., Sifeddine, A., Le Forestier, L., 2016. Organic matter-clay interaction along a seawater column of the Eastern Pacific upwelling system (Antofagasta bay, Chile): implications for source rock organic matter preservation. Marine Chemistry 179, 23-33.

503 Mahamat-Ahmat, A., Boussafir, M., Le Milbeau, Guégan, R., De Oliveira, T., Le Forestier,
504 L., 2017. Organic matter and clay interaction in a meromictic lake: implications for
505 source rock OM preservation (Lac Pavin, Puy-de-Dôme, France). Organic
506 Geochemistry 109, 47-57.

507 Meleshyn, A., Tunega., 2011. Adsorption of phenanthrene on Na-Montmorillonite: A model
508 study. Geoderma 169, 41-46.

509 Nam Jang, B., Wilkie, C.A., 2004. A TGA/FTIR and mass spectral study on the thermal
510 degradation of bisphenol A polycarbonate. Polymer Degradation and Stability 86, 419-
511 430.

512 Özcan, A.S., Erdem, B., Özcan, A., 2005. Adsorption of acid blue 193 from aqueous solutions
513 onto BTMA-bentonite. Colloids and Surfaces A: Physicochemical and Engineering
514 Aspects 266, 73-81.

515 Patzko., A., Decany., I., 1993 Ion exchange and molecular adsorption of a cationic surfactant
516 on clay minerals . Colloids and Surfaces A: Physicochemical and Engineering Aspects.
517 71 (1993) 299-307.

518 Plante, A.F., Pernes, M., Chenu, C., 2005. Changes in clay-associated organic matter quality
519 in a C depletion sequence as measured by differential thermal analyses. Geoderma 129,
520 186-199.

521 Rabiei, M., Sabahi, H., Rezayan, A.H., 2016. Gallic acid-loaded montmorillonite
522 nanostructure as a new controlled release system. Applied Clay Science 119, 236-242.

523 Rao, C.R.M., Reddy, V.B., Mehrotra, P.N., 1981. Derivatographic studies of gallic acid.
524 Thermochimica Acta 46, 65-69.Shainberg, I., Oster, J.D., Wood, J.D., 1980. Sodium /
525 Calcium Exchange in Montmorillonite and Illite Suspensions 1, Soil Science Society of
526 America Journal 44, 960–964.

527 Swartzen-Allen, S.L., Matijević, E., 1975. Colloid and surface properties of clay suspensions:
528 II. Electrophoresis and cation adsorption of montmorillonite. Journal of Colloid
529 Interface Science 50, 143–153.

530 Sonon, L.S., Thompson, M.L., 2005. Sorption of a nonionic polyoxyethylene lauryl ether
531 surfactant by 2:1 layer silicates. Clays and Clay minerals 53, 45-54.

532 Schmidt, M.W.I., Torn, M.S., Abiven, S., Dittmar, T., Guggenberger, G., Janssens, I.A.,
533 Kleber, M., Kögel-Knabner, I., Lehmann, J., Manning, D.A.C., Nannipieri, P., Rasse,
534 D.P., Weiner, S., Trumbore, S.E., 2011. Persistence of soil organic matter as an
535 ecosystem property. Nature 478, 49-56.

536 Stevenson, F.J. 1982. Humus Chemistry. John Wiley & Sons, New York.

537 Theng, B.K.G., Aslabie, J., Fraser, R., 2001. Bioavailability of phenanthrene intercalated into
538 an alkylamonium-montmorillonite clay. Soil Biology and Biogeochemistry 33, 845-848.

539 Thiebault, T., Guégan, R., Boussafir, M., 2015. Adsorption mechanisms of emerging micro-
540 pollutants with a clay mineral: case of tramadol and doxepine pharmaceutical products.
541 Journal of Colloid and Interface Science 453, 1-8.

542 Thiebault, T., Boussafir, M., Guégan, R., Le Milbeau, C., Le Forestier, L., 2016. Clayey-sand
543 filter for the removal of pharmaceuticals from wastewater effluent: percolation
544 experiments. Environmental Science Water Research & Technology 2, 529-538.

545 Tombácz, E., Libor, Z., Illés, E., Majzik, A., Klumpp, E., 2004. The role of reactive surface
546 sites and complexation by humic acids in the interaction of clay mineral and iron oxide
547 particles. Organic Geochemistry 35, 257-267.

548 Tombácz, E., Szekeres, M., 2006. Surface charge heterogeneity of kaolinite in aqueous
549 suspension in comparison with montmorillonite. Applied Clay Science 34, 105-124.

550 Wang, K., Xing., B., 2005. Structural and sorption characteristics of adsorbed humic acid on
551 clay minerals. Journal of Environmental Quality, 34 342-349.

552 Wang, T.S.C., Wang, M.C., Ferng, Y.L., 1983. Catalytic synthesis of humic substances by
553 natural clays, silts, and soils. Soil Science 135, 350-360.

554 Wattel-Koekkoek, E.J.W., Buurman, P., 2004. Mean residence time of kaolinite and smectite-
555 bound organic matter in Mozambiquan soils. Soil Science Society of America Journal
556 68, 154-161.

557 Williams, D.J.A., Williams, K.P., 1978. Electrophoresis and zeta potential of kaolinite.
558 Journal of Colloid and Interface Science 65, 79-87.

559 Xie, W., Gao, Z., Liu, K., Pan, W.-P., Vaia, R., Hunter, D., Singh, A., 2001. Thermal
560 characterization of organically modified montmorillonite. Thermochimica Acta 367-
561 368, 339-350.

562 Yan, L., Wang, J., Yu, H., Wei, Q., Du, B., Shan, X., 2007. Adsorption of benzoic acid by
563 CTAB exchanged montmorillonite. Applied Clay Science 37, 226-230.

564 Yariv, S., Cross, H., 2002. Organo-clay complexes and interactions. Marcel Dekker, New
565 York 688pp.

566 Zhang, L., Luo, L., Zhang, S., 2012. Integrated investigations on the adsorption mechanisms
567 of fulvic and humic acids on three clay minerals. Colloids and Surfaces A:
568 Physicochemical and Engineering Aspects 406, 84-90.

569 Zhu, J., Zhang, P., Qing, Y., Wen, K., Su, X., Ma, L., Wei, J., Liu, H., He, H., Xi, Y., 2017.
570 Novel intercalation mechanism of zwitterionic surfactant modified montmorillonites.
571 Applied Clay Science 141, 265- 271.

572

573

Highlights

- Gallic acid (GA) adsorption onto Na-Mt was performed in batch conditions;
- Data were fitted to Dubinin-Radushkevitch, Langmuir and Freundlich equations;
- Following the acidity, both edge and interlayer interactions modes were observed;
- GA intercalates under its neutral form;

Table 1

Click here to download Table: Table 1.docx

	Properties	Values
Na-MMt	C.E.C ($mol.g^{-1}$)	8.10^{-4}
	p_{znc}	4.5
GA	COOH pKa	4.4
	Surface area ($Å^2$)	98

Table 2

Click here to download Table: table 2.docx

		Langmuir					Freundlich				Dubinin-Radushkevich			
		q_{max} ($mol.g^{-1}$)	K_L (L.mol)	ΔG (kJ.mol)	r^2	F_{error}	K_F ($L.g^{-1}$)	n	r^2	F_{error}	q_{max} ($mol.g^{-1}$)	E ($kJ.mol^{-1}$)	r^2	F_{error}
Gallic Acid	pH 2	2.12×10^{-4}	1.2×10^{3}	-17.40	0.961	0.176	1.02×10^{-3}	3.08	0.960	3×10^{-3}	3.64×10^{-4}	11.04	0.964	4×10^{-3}
	pH 5	1.19×10^{-4}	1.4×10^{3}	-18.00	0.977	0.199	4.87×10^{-4}	3.50	0.976	7×10^{-4}	2.51×10^{-4}	7.88	0.963	2.0×10^{-3}
	pH 7	1.52×10^{-4}	5.8×10^{2}	-15.77	0.977	0.034	1.33×10^{-3}	1.78	0.981	1×10^{-4}	3.51×10^{-4}	7.76	0.988	1.5×10^{-3}

Figure 1
Click here to download Figure: Fig1.pdf

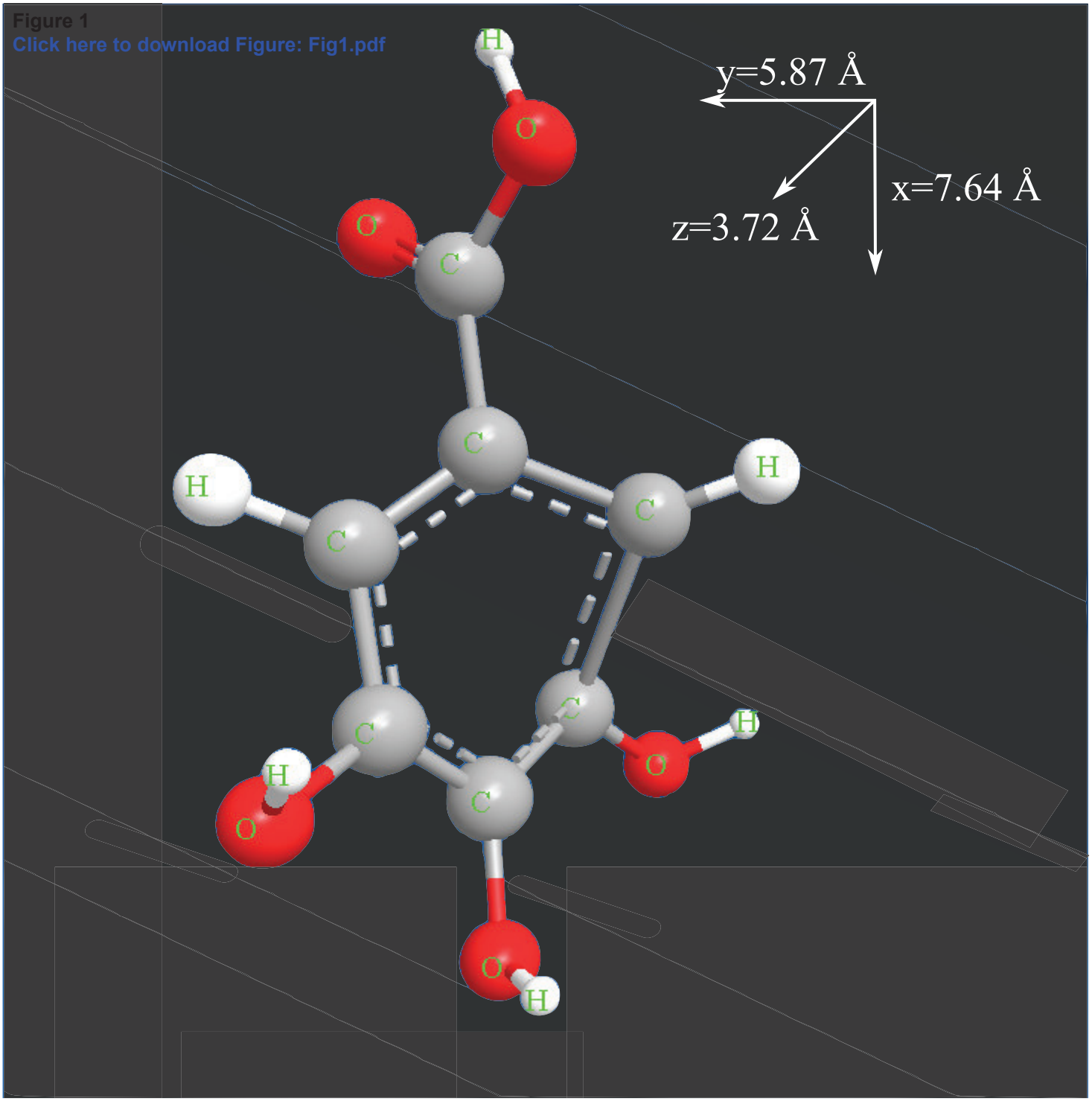

Figure 2

Click here to download Figure: Fig 2.PDF

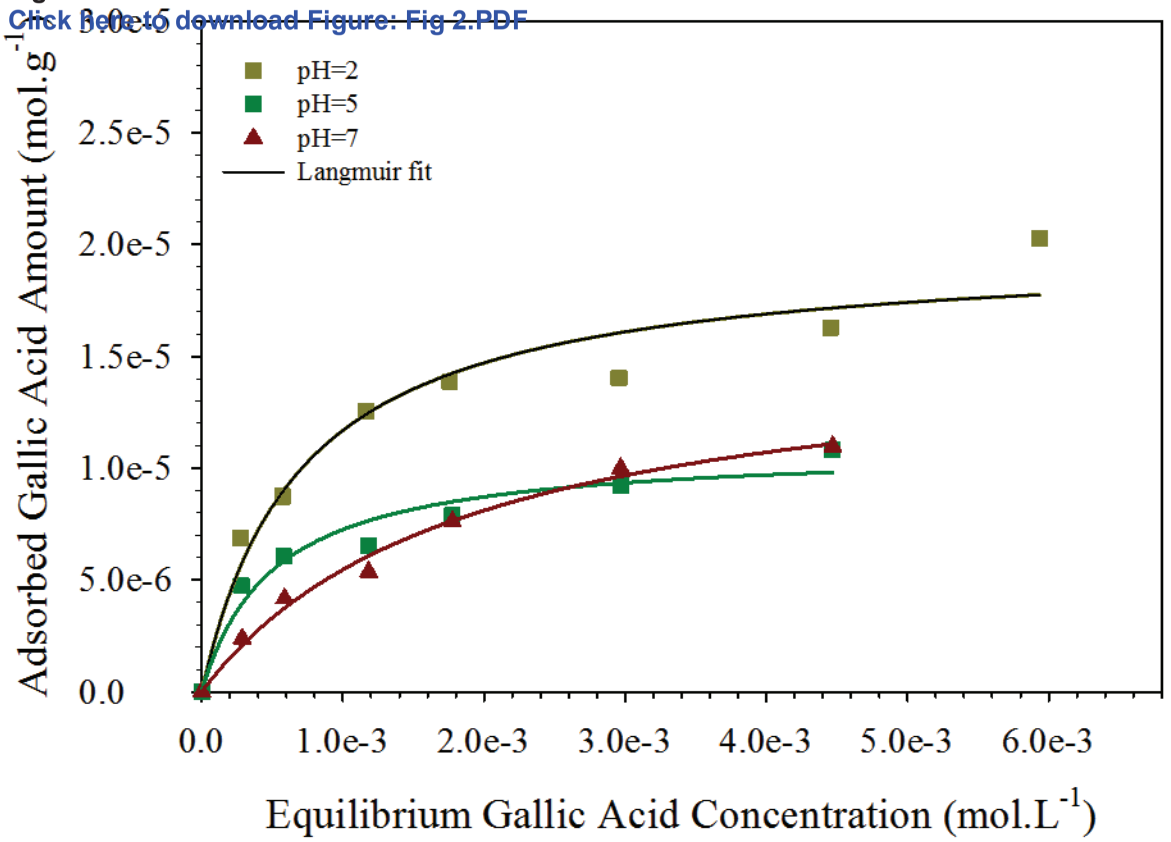

Figure 3

Click here to download Figure: Fig3.pdf

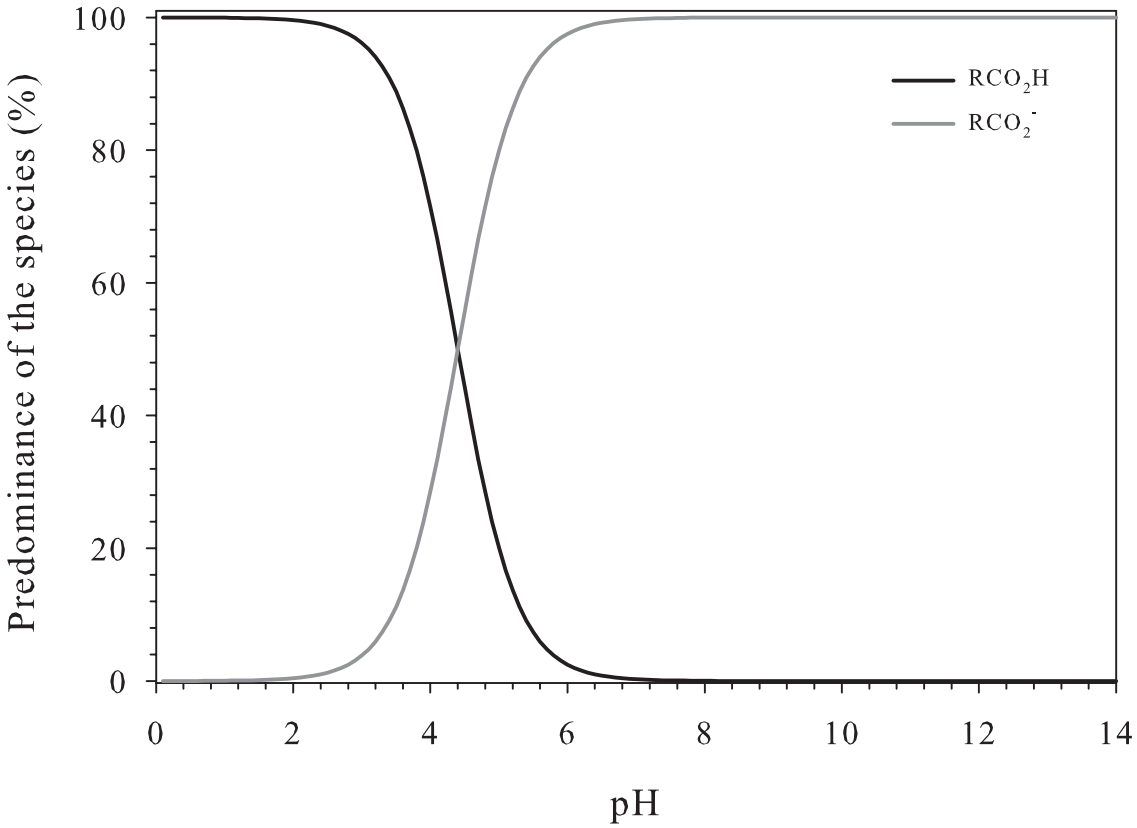

Figure 4
Click here to download Figure: Fig 4.PDF

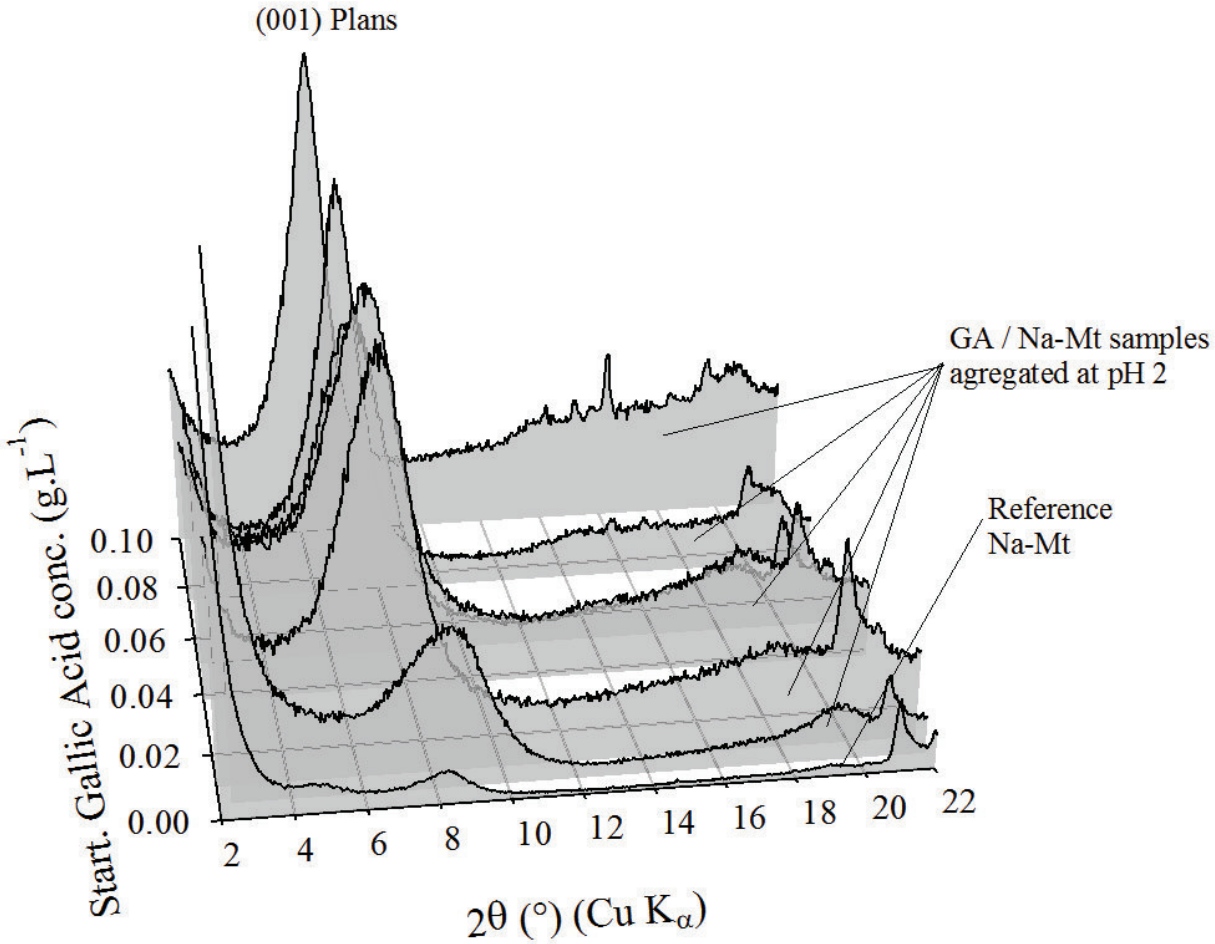

Figure 5

Click here to download Figure: Fig5.pdf

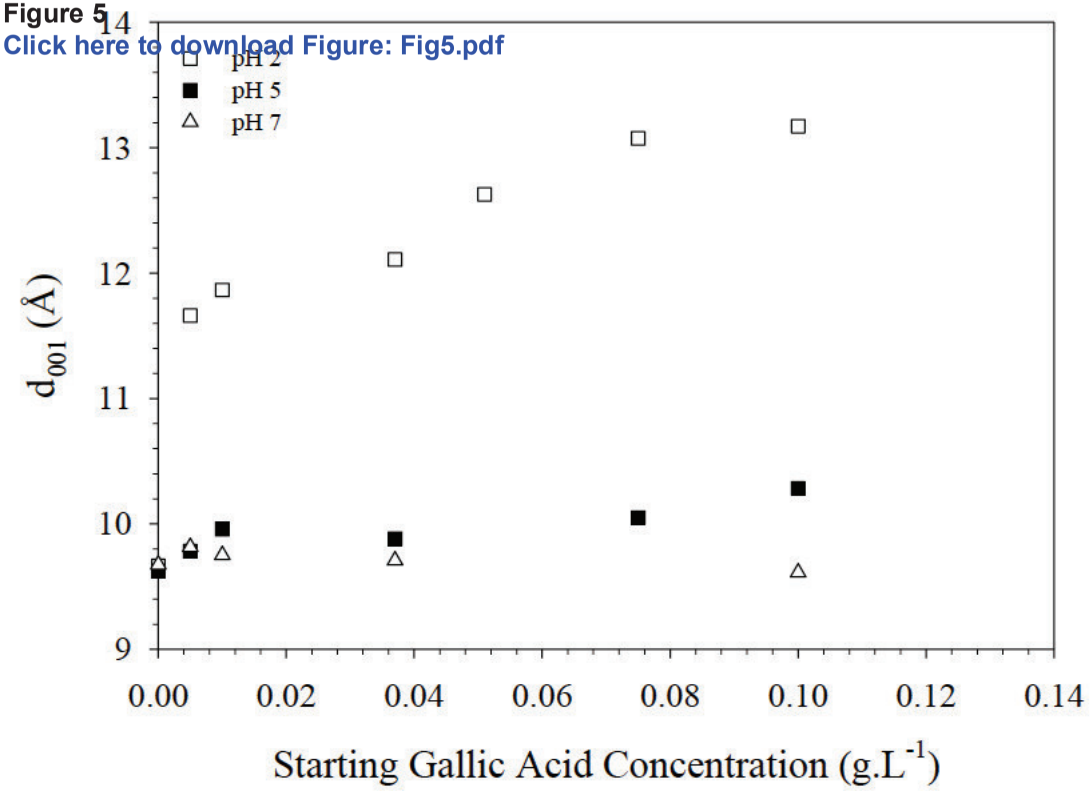

Figure 6
Click here to download Figure: Fig 6.PDF

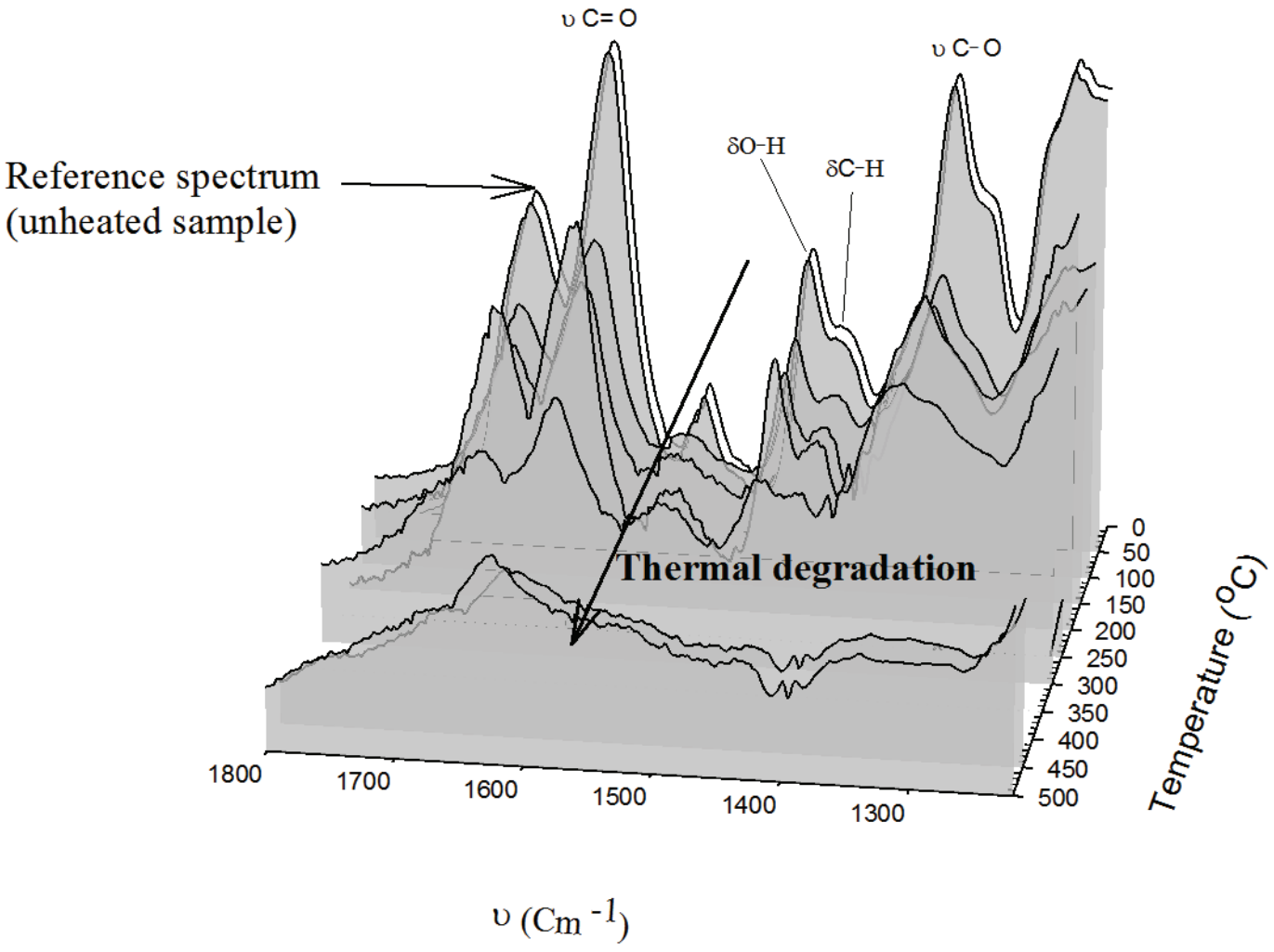

Figure 7
Click here to download Figure: Fig 7.pdf

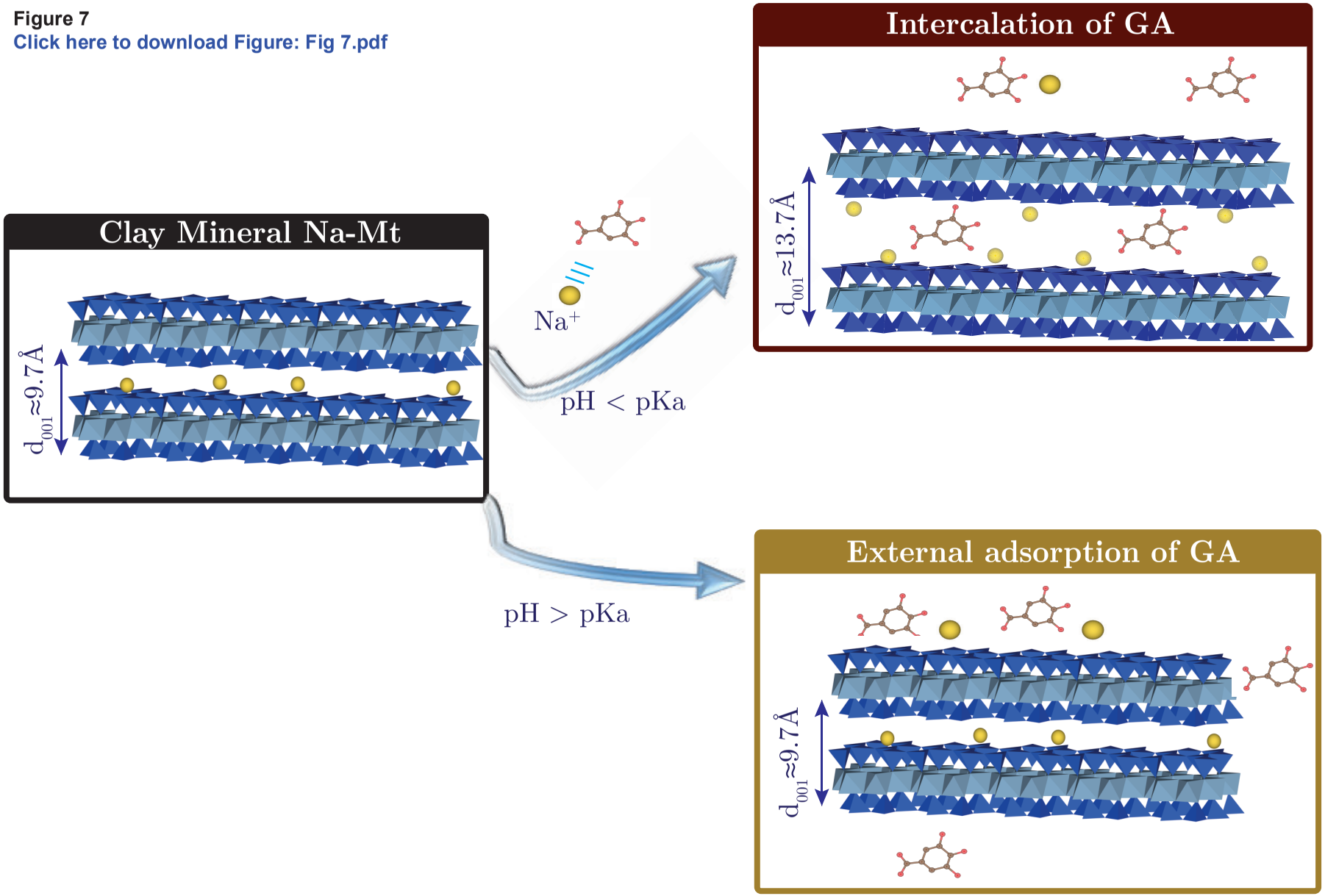

Figure 8

Click here to download Figure: Fig8.pdf